Available online at www.sciencedirect.com
ScienceDirect
Catalysis Today 118 (2006) 288–297
CATALYSIS TODAY
www.elsevier.com/locate/cattod

Kinetic parameter estimation for supported vanadium oxide catalysts for propane ODH reaction: Effect of loading and support

Debaprasad Shee, T.V. Malleswara Rao, Goutam Deo *

Department of Chemical Engineering, Indian Institute of Technology Kanpur, Kanpur 208016, India

Available online 22 August 2006

Abstract

Kinetic parameters are estimated for a sequential Mars van Krevelan (MVK) reaction model occurring over several supported vanadium oxide (vanadia) catalysts involved in the propane oxidative dehydrogenation (ODH) reaction. The estimated kinetic parameters, pre-exponential factors and activation energies, are used to understand the effect of vanadia loading and oxide support. The pre-exponential factors and vanadia normalized pre-exponential factors vary with vanadia loading and oxide support. The monotonic increase in normalized pre-exponential factors with vanadia loading and the variation of pre-exponential factors with oxide support appears to be related to the change in acidity/basicity of the catalyst and the redox nature of the catalyst, respectively. The activation energy for propene degradation does not significantly change with catalyst; however, the activation energy for propane oxidation is different for the V_2O_5/Al_2O_3 catalyst. It appears that two important considerations are required for the development of an efficient propane ODH catalyst: a high rate constant associated with the propane oxidation reaction, and a high ratio of the rate constant for propene formation to degradation reaction. Based on the observations in the present study it is proposed that a higher TiO_2 support surface area will assist in increasing the propane oxidation activity and propene yield.

Keywords: Kinetic parameters; ODH reaction; Mars van Krevelan (MVK) reaction model; Supported vanadium oxide catalysts

1. Introduction

The primary objective in the oxidative dehydrogenation (ODH) of propane reaction is to simultaneously increase the propane oxidation activity and propene yield with the proper choice of a catalyst. The activity is improved by choosing a catalyst that shows high conversion and the propene yield is improved by tuning the inverse selectivity versus conversion curve of the catalyst that is commonly observed. The ODH of propane to propene has been extensively studied over supported vanadia catalysts [1–4 and references therein]. In the propane ODH and several other reactions involving partial oxidation over supported vanadia catalysts it was determined that the vanadia loading and oxide supports are important parameters to consider for the design of the catalysts [5–12]. Some of the studies that are specifically targeted at studying the effect of vanadia loading and TiO_2 or Al_2O_3 oxide supports for propane ODH are those by Arena et al. [5], Lemonidou et al. [6], Martra et al. [7], Khodakov et al. [8], Chen et al. [9] and Routray et al. [10]. In these studies it was observed that the propane oxidation activity increases with vanadia loading up to about monolayer coverages and decreases thereafter. Below monolayer coverages only surface vanadia species are present and above monolayer coverages bulk V_2O_5 is formed. Thus, the surface vanadia species were proposed to be more active for the propane ODH reaction. The propane ODH reactivity also depends on the oxide support used to form the surface vanadia species. For example, in terms of specific propane ODH activity the surface vanadia site on TiO_2 support is more suitable than the surface site on Al_2O_3 [6,7,10].

Only a few studies exists that are aimed at understanding the effect of vanadia loading and oxide support by analysis of the kinetic parameters involved in the propane ODH reaction. For example, using pseudo-first order reaction mechanisms Bell, Iglesia and co-workers observed variations in rate constant ratios and activation energy changes for several supported vanadia catalysts [8]. Bottino et al. [13] used a power law and Anderson [14] used a Rideal type rate expression for describing the kinetics of propane ODH. Grabowski et al. [15] studied kinetics of propane ODH over V_2O_5/TiO_2 catalyst considering

* Corresponding author. Tel.: +91 512 2597881; fax: +91 512 2590104.
E-mail address: goutam@iitk.ac.in (G. Deo).

0920-5861/$ – see front matter © 2006 Elsevier B.V. All rights reserved.
doi:10.1016/j.cattod.2006.07.017

pseudo-homogeneous and steady state adsorption model. Furthermore, most of these studies only consider the amount of propene formed while estimating and applying the kinetic parameters, and do not involve an analysis of all reaction products.

Kinetic parameters can assist in comparing the catalytic differences associated with the propane ODH reaction. Important in the estimation of the kinetic parameters is the specific reaction model. Recently, it has been shown that the complete description of the reactants and products is possible with the help of a Mars van Krevelan (MVK) reaction model and the kinetic parameters estimated for this reaction model are reliable [10,16,17]. The reaction parameters are estimated with the help of a genetic algorithm (GA) that optimizes a determinant based objective function involving the inlet and outlet concentrations of all carbon containing gases.

The present study uses the MVK reaction model to understand the effect of vanadia loading and oxide support in terms of the kinetic parameters estimated. The effect of vanadia loading is determined by using three different vanadia loading for the vanadia–titania (V_2O_5/TiO_2) catalyst. The effect of oxide support is determined by using three different commercially available supports: titania (TiO_2), alumina (Al_2O_3) and niobia (Nb_2O_5). The catalysts are initially characterized by determining the surface areas and by Raman spectroscopy. Propane ODH reactions are then carried out to observe the effect of vanadia loading and oxide support on the activity and selectivity and for estimation of the kinetic parameters involved in this reaction. The kinetic parameters are then compared to understand the effect of vanadia loading and oxide support. Finally, suggestions are offered to improve the propane oxidation activity and propene yield.

2. Experimental

2.1. Catalyst synthesis

A series of vanadium oxide supported on TiO_2 catalysts were prepared by incipient wetness impregnation method to understand the effect of loading on the kinetic parameter. For understanding the effect of support two vanadium oxide catalyst samples supported on alumina and niobia were also considered. For the vanadia–alumina system a 10% V_2O_5 loading and for the vanadia–niobia system a 7% V_2O_5 loading was used. The synthesis of the 7% V_2O_5/Nb_2O_5 sample has been described elsewhere [18]. The vanadia precursor used for the synthesis of V_2O_5/TiO_2 and V_2O_5/Al_2O_3 catalysts was ammonium meta-vanadate (NH_4VO_3, 98% purity) and the supports used were titania (Degussa, P25) and alumina (Condea). The TiO_2 and Al_2O_3 supports used in this present study were pretreated with incipient volume of oxalic acid solution [10]. During preparation of the vanadia precursor solution a calculated amount of powdered ammonium meta-vanadate was added to a solution containing stoichiometric amounts of oxalic acid. The total volume of the solution was similar to the incipient-wetness impregnation volume of the support. The resulting mixture was thoroughly stirred till complete dissolution of the solids. The deep blue solution obtained was intimately mixed with the pretreated support to form a paste. The pastes were then kept in desiccators for drying at room temperature for 8 h and at 383 K for 6 h. Finally the catalysts were calcined at 723 K for the vanadia–titania samples, at 773 K for the vanadia–niobia sample and at 873 K for the vanadia–alumina sample. The final calcinations temperatures were different due to the different thermal stability of the supported vanadia catalysts and were always greater than the reaction temperatures.

2.2. Surface area measurement

The surface area of all the catalyst samples was determined by nitrogen adsorption method using BET multi point equation. The apparatus used for these studies was COULTER SA 3100 analyzer equipped with SA-VIEW^{TM} software. Degassing of the samples was achieved by heating the samples at 423 K in flowing helium.

2.3. Raman spectroscopy

The catalysts were characterized by laser Raman spectroscopy under ambient and dehydrated conditions. The spectra were obtained using a Raman spectrometer system (JY-Horbia LabRam HR) with a confocal microscope, 2400/900 grooves/mm grating and a notch filter. The samples were excited with a 532 nm Ar laser and the spectral resolution was $\sim$2 cm^{-1}. The scattered photons were directed into a single monochromator and a LN_2 CCD detector (Spex) was used to collect the signal. The powdered samples were placed in an *in situ* cell (Linkam, TS-1500), which allows temperature treatments up to 1773 K under flowing gases. To obtain spectra under dehydrated conditions the samples were pretreated *in situ* in an O_2 + He gas flow at 673 K for 0.5 h [19].

2.4. Reaction studies

The propane ODH reaction was carried out in a fixed-bed, down-flow, plug-flow isothermal quartz reactor at atmospheric pressure. The reactor was made by fusing two quartz tube of length 150 mm each. The diameter of inlet and outlet section was kept 10 and 4 mm respectively. The catalyst bed of 1 cm length was made by mixing measured amount of catalyst sample and hydrofluoric acid pretreated quartz particle and the bed was supported on quartz wool. The quartz particles had to be pretreated and pre-calcined at 1073 K to ensure no reaction. The reactor was placed vertically in the tubular furnace. The temperature of catalyst bed was measured by inserting a thermocouple inside the quartz reactor. A PID controller (FUJI micro controller-PXZ4) was used to control the temperature of the bed within $\pm$1 K of the set value. The product gases taken out from the bottom of the reactor were sent for online analysis to a gas chromatograph (AIMIL NUCON-5700) equipped with methanizer. The product gases (carbon oxides and propene) and unreacted propane were analyzed in a FID mode using a Hysep-Q column.

The reactant gases (C_3H_8, N_2 and O_2) flow rates were controlled separately by three electronic mass flow controllers (Bronkhost Hi-Tech, E1-flow mass flow controller). Contact time studies were carried out at 653 K using propane to oxygen molar ratio of 2:1. For kinetic parameter estimation, the propane to oxygen molar ratio was varied from 1:1 to 3:1 and temperature was varied from 613 to 673 K. Nitrogen was used as a diluent and its amount was fixed corresponding to air composition. The total flow rate of reactant gas mixture was kept at 75 ml/min for kinetic parameter estimation studies. The propane conversion was maintained below 10% for all reactivity studies to ensure differential reactor condition. Blank experiments were also carried out under same reaction conditions to ensure no contribution of homogeneous reaction to the net reaction.

2.5. Kinetic parameter estimation

Several assumptions are considered in developing the mathematical model for a plug flow reactor containing the catalyst [16]. These assumptions are justified since low propane conversions are maintained and nitrogen and inert quartz particles are used as diluents. Based on these assumptions the differential material balance equation for each component, i, in a plug flow reactor is

$$\frac{dx_i}{dW} = \frac{\sum_j n_{ij} r_j}{V_0} \tag{1}$$

where x_i is mole fraction of the ith component; W weight of the catalyst; n_{ij} stoichiometric coefficient of the ith component for the jth reaction; r_j rate of jth reaction; V_0 is volumetric flow rate of the feed.

The set of ordinary differential equations given in Eq. (1) can be solved to obtain the predicted output mole fraction of each component based on the input mole fraction of the component, x_{i0}, and knowledge of r_j, W, n_{ij}, V_0, temperature and pressure of the reaction. The reaction rate, r_j, depends on the specific reaction-model considered. The reaction rate contains several non-linear kinetic parameters, θ_j, and some or all mole fractions, x_i, and is described below. Thus, the predicted output mole fractions are obtained by integrating the reaction rates over the entire mass based on a chosen reaction mechanism. A fourth order Runge-Kutta method is employed for the integration of rate expressions.

The output mole fraction of carbon containing compounds that are detected, C_3H_8, C_3H_6, CO and CO_2, are assumed to be well represented by a non-linear model given by

$$Y_h = g_h(\theta, X) + Z_h, \quad h = 1, 2, \ldots, v \tag{2}$$

where Y_h is vector of random variables representing the response or the observed output variable; $g_h(\theta,X)$ predicted output concentration; θ parameter vector; X vector of experimental variables (i.e., input mole fractions of components and temperature); Z_h is vector of errors associated while calculating the response.

The predicted output mole fraction g_h obtained this way can then be compared with the actual output mole fraction Y_h based on the kinetic parameter values.

For multi-response systems and when responses are correlated, minimization of a determinant is ideally suited for comparing the predicted and actual output mole fractions [20–24]. During the minimization process the kinetic parameters are chosen such that the least value of the determinant is obtained [20].

The determinant that is minimized for multiresponse systems

$$= |Z_{hk}| \tag{3}$$

where

$$Z_{hk} = \sum_{u=1}^{n} (y_{hu} - g_{hu})(y_{ku} - g_{ku}); \quad h \text{ and } k = 1, \ldots, v \tag{4}$$

n is number of experiments; v number of responses; y_{hu} experimental mole fraction of hth component in uth experiment; g_{hu} is predicted mole fraction of hth component in uth experiment.

In the present study minimization of the objective function given by Eq. (3) is achieved by applying a GA for determining the kinetic parameters. The GA uses a tournament selection operator with real coded fixed-boundary variables. Furthermore, simulated binary crossover and polynomial mutation are used for these real coded variables. Additional details can be found elsewhere [25]. The parameters used in the GA code are listed in Table 1.

The number of kinetic parameters involved in the set of r_j's depend on the particular reaction model chosen. Several models have been proposed for the propane ODH reaction. Among them, the Mars van Krevelen (MVK) model has been widely accepted as the most suited for the propane ODH reaction over supported vanadium oxide catalysts [15,16]. For the purpose of understanding the effect of the vanadia loading and the oxide support, a simplified MVK model considering propene (C_3H_6) as primary and carbon oxides ($CO_x = CO + CO_2$) as secondary products is used in the present study. The MVK mechanism chosen for this study assumes that the propane molecules react with lattice oxygen of the catalyst to produce propene molecules, which then further reacts with lattice oxygen to produce carbon oxides. The gas phase oxygen replenishes the lattice oxygen by re-oxidation of the catalyst. It was observed that for each catalyst a specific CO_2 to CO molar ratio was

Table 1
GA parameters used in the present study

GA parameters	Values for MVK models
Generations	5000–50000
Population size	80–150
Crossover probability	0.9
Mutation probability	0.1
Tournament size	2
Exponent for simulated binary crossover	2
Exponent for mutation	200
Seed value	0.123–0.2

present over the entire experimental conditions. Thus, a constant ratio between the numbers of moles of CO_2 to CO, ψ, is used to simplify analysis. The three reactions, r_1, r_2 and r_3 considered are given below.

1. Formation of propene (r_1) or propane oxidation:
   The gas phase propane reacts with lattice oxygen forming gas phase propene.

$$C_3H_8(g) + O(s) \rightarrow C_3H_6(g) + H_2O + *_{red} \quad (5)$$

   where $*_{red}$ is a reduced site.
2. Formation of CO_x or propene degradation (r_2):
   The gas phase propene reacts with lattice oxygen to form gas phase CO_x.

$$C_3H_6(g) + 3(x+1)O(s) \rightarrow 3CO_x(g) + 3H_2O + 3(x+1)*_{red} \quad (6)$$

   where x is 1 for CO and 2 for CO_2
3. Catalyst re-oxidation (r_3):
   Finally, the reduced catalyst is re-oxidized by gas phase oxygen.

$$O_2(g) + 2*_{red} \rightarrow 2O(s) \quad (7)$$

The rate expressions for the above three reactions, Eqs. (5)–(7), are expressed as

$$r_1 = k_1 P_{C_3H_8}(1-\beta) \quad (8)$$

$$r_2 = k_2 P_{C_3H_6}(1-\beta) \quad (9)$$

$$r_3 = k_3 P_{O_2}\beta \quad (10)$$

where k_j is the rate constant for the jth reaction, in ml STP min^{-1} (g cat)$^{-1}$ atm^{-1}; P_i the partial pressure of the component, i, in atm; β is the degree of reduction of the catalyst, which is dimensionless.Thus, the gas phase propane reacts with lattice oxygen to form propene, Eq. (5), with a rate constant k_1. Propene is further oxidized to CO_x, Eq. (6), with a rate constant k_2. Catalyst re-oxidation of the reduced sites, Eq. (7), occurs with a rate constant k_3. Consequently, there are six kinetic-parameters in total that need to be estimated; a k_{i0} and E_i associated with each k_i. Furthermore, assuming that the rate of lattice-oxygen consumed in the reactions r_1 and r_2 is equal to the rate of lattice-oxygen replacement by the reaction r_3, β can be expressed as

$$\beta = \frac{0.5k_1P_{C_3H_8} + (3(3\psi+2))/(2(\psi+1))k_2P_{C_3H_6}}{0.5k_1P_{C_3H_8} + (3(3\psi+2))/(2(\psi+1))k_2P_{C_3H_6} + k_3P_{O_2}} \quad (11)$$

In chemical kinetics high correlations are frequently encountered between estimates of the parameters in the Arrhenius expression for a rate constant making the elucidation of a reaction network very difficult [26–28]. To overcome the correlation between parameters re-parameterization is required. Re-parameterization is achieved by reformulating the rate constants in the present study as

$$k_i = k_{i0}\exp\left[\frac{-E_i}{R}\left(\frac{1}{T}-\frac{1}{T_m}\right)\right] \quad (12)$$

where k_{i0} is pre-exponential factor (ml STP min^{-1} (g cat)$^{-1}$ atm^{-1}); E_i activation energy for the reaction i (kJ/mol); T actual reaction temperature (K); R universal gas constant (kJ (kmol)$^{-1}$ K); T_m is mean temperature (K).

This type of centering eases the parameter search by minimizing the statistical correlation between the activation energy and pre-exponential factor [26,27]. Standard error calculations of the kinetic parameters, k_{i0}'s and E_i's, are achieved by applying previously defined equations [16,17].

3. Results and discussion

The particulars of the supported vanadia catalysts are listed in the first three columns of Table 2. The last column of Table 2 gives the CO_2 to CO ratio, ψ, over the entire experimental conditions and is discussed later. Examination of Table 2 reveals that the surface area of the synthesized catalyst is not significantly affected, except for the 10VAl sample, where the surface area decreased from 180 to 146 m^2/g. Such a decrease in surface area has been observed previously [10] and is usually associated with the decrease in the micropores and/or the difference in the atomic weights of vanadium and aluminum. XRD patterns of the supported vanadium oxide catalysts only reveal features of the support and are not shown for brevity. No changes are observed in the XRD bands of the oxide support. Thus, the support appears to be unaffected after the catalyst preparation.

Table 2
Particulars of the catalyst samples

Nomenclature	V_2O_5 (wt.%)	Surface area (m^2/g)	Surface density (V atoms/nm^2)	CO_2/CO[a], ψ
TiO2	–	46	–	–
1VTi	1	49	1.4	0.72
2VTi	2	41	3.2	0.61
3VTi	3	43	4.6	0.52
Al_2O_3	–	180	–	–
10VAl	10	146	4.5	0.68
Nb_2O_5	–	55	–	–
7VNb	7	51	9.1	0.57

[a] Based on entire reaction data.

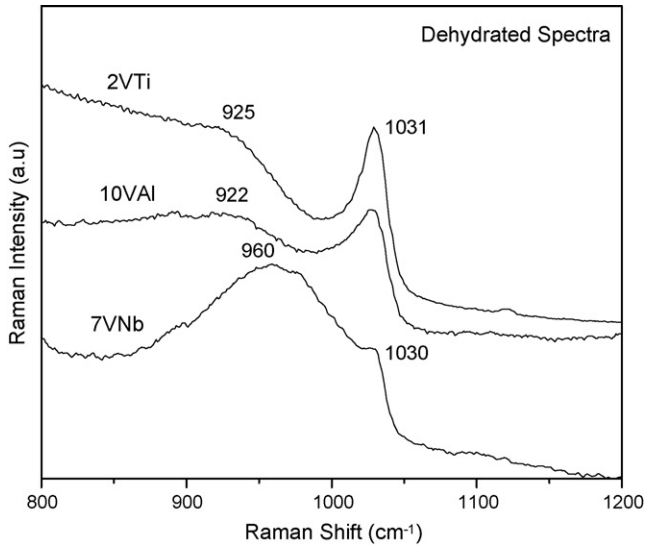

Fig. 1. Raman spectra of 2VTi, 10VAl and 7VNb catalysts under dehydrated conditions.

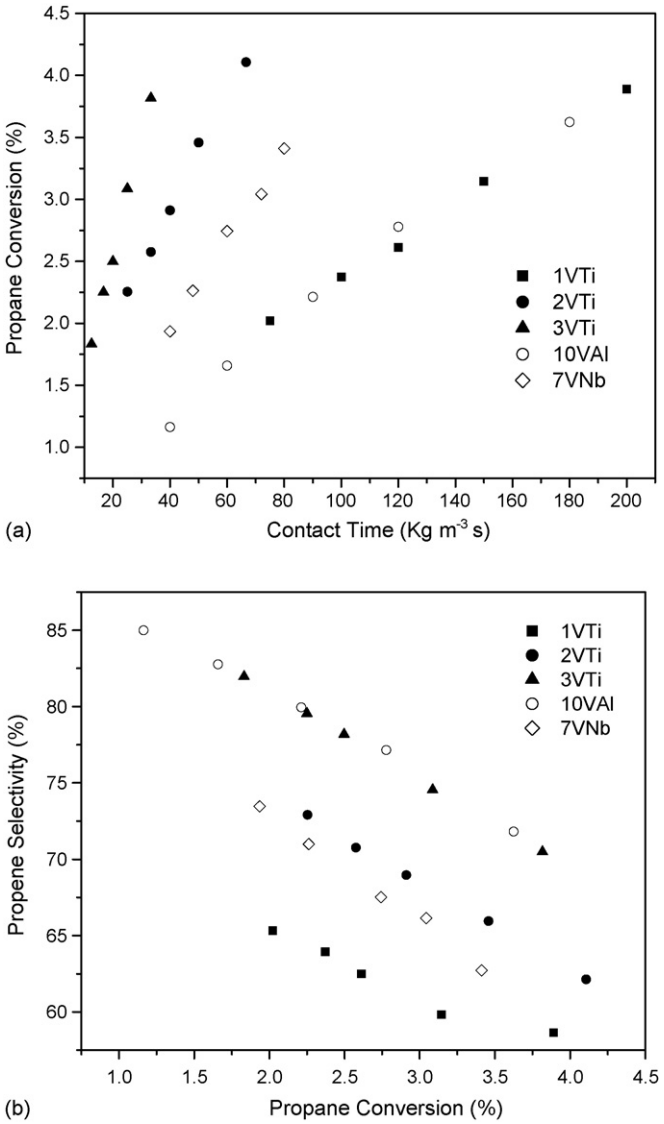

Fig. 2. (a) Propane conversion as a function of contact time for the different supported vanadia catalysts. $T = 653$ K and $C_3H_8{:}O_2 = 2{:}1$. (b) Propene selectivity vs. conversion for the different catalysts. $T = 653$ K and $C_3H_8{:}O_2 = 2{:}1$.

The Raman spectra of the five catalyst samples under ambient and dehydrated conditions were obtained. The spectra of the catalysts under ambient conditions reveal Raman features due to surface vanadium oxide species and are not shown for brevity. The Raman spectra of 2VTi, 10VAl and 7VNb obtained under dehydrated conditions are shown in Fig. 1 in the 800–1200 cm^{-1} region and reveal features due to molecularly dispersed vanadia species. Raman bands are observed at $\sim$1030 cm^{-1} due to the terminal V=O bond vibration and at 920–960 cm^{-1} due to polymeric or support associated vanadia bonds [8,29–32]. Several previous studies have been conducted to elucidate the structure of the surface vanadium oxide species [33–37]. These results suggest that essentially two types of molecularly dispersed surface vanadium oxide species are present. The first species is monomeric and is predominantly present at low surface coverages and the second species is polymeric and is predominantly present at high surface coverages. The present study does not intend to address the nature of the apparent different vanadia structures, but is aimed at confirming that only surface vanadia species are present on the oxide supports.

The propane ODH reaction was initially carried out over the five catalysts as a function of contact time. The propane conversion as a function of contact time is shown in Fig. 2a. With an increase in contact time an increase in conversion is observed. It is also clear from Fig. 2a that at a particular contact time the propane conversion is a function of loading and oxide support. At a particular contact time, increasing the vanadia loading from 1 to 3% V_2O_5 increases the propane conversion. Furthermore, as the support is changed the propane conversion is also affected and for a particular contact time the trend in propane conversion of the five catalysts is: 3VTi > 2VTi > 7VNb > 10VAl $\sim$ 1VTi. Using the propane conversion data the turnover frequency (TOF), defined in terms of propane moles converted per vanadia site per unit time, is calculated. As a function of loading the ratio of the experimentally determined propane oxidation TOF at an interpolated/extrapolated contact time of 75 kg m^{-3} s is $(TOF)_{1VTi}{:}(TOF)_{2VTi}{:}(TOF)_{3VTi} \sim 1{:}1.1{:}1.1$, suggesting that the TOF is relatively independent of coverage. Wachs and co-workers [12,18,38] and Eon et al. [39] have observed relatively similar TOF values with increase in loading for the vanadium oxide species on different oxide supports suggesting that the propane oxidation reaction is structure insensitive. Furthermore, the propane oxidation TOF for all the catalysts at a contact time of 75 kg m^{-3} s is $(TOF)_{10VAl}{:}(TOF)_{7VNb}{:}(TOF)_{1VTi}{:}(TOF)_{2VTi}{:}(TOF)_{3VTi} \sim 1{:}2.4{:}10.5{:}11.6{:}11.7$, which suggests that the TOF is a strong function of the oxide support used to form the surface vanadia species and varies by an order of magnitude as the support is changed from Al_2O_3 to TiO_2. Previous studies also reveal that the propane activities are functions of oxide support used to form the surface vanadia species [6–8]. The propene selectivities as a function of conversion for the five catalysts are shown in Fig. 2b. As expected an inverse relationship between

Table 3
Kinetic parameter values of the supported vanadia catalysts

Parameter (units)	Catalysts				
	1VTi	2VTi	3VTi	7VNb	10VAl
k_{10} (ml STP min^{-1} (g cat) $^{-1}$ atm^{-1})	11.5 (1)	40 (2)	87 (6)	27 (1)	17 (1)
k_{20} (ml STP min^{-1} (g cat) $^{-1}$ atm^{-1})	379 (14)	739 (64)	1488 (117)	525 (3)	232 (10)
k_{30} (ml STP min^{-1} (g cat) $^{-1}$ atm^{-1})	93 (9)	345 (54)	540 (96)	661 (8)	396 (11)
k_{10}/k_{20}	0.030	0.054	0.059	0.051	0.073
E_1 (kJ mol^{-1})	73 (5)	70 (5)	65 (4)	68 (1)	96 (2)
E_2 (kJ mol^{-1})	53 (5)	43 (9)	47 (6)	47 (1)	58 (2)
E_3 (kJ mol^{-1})	136 (11)	144 (13)	136 (15)	171 (4)	114 (13)
$E_1 - E_2$ (kJ mol^{-1})	20	27	18	21	38

Standard errors are given in parenthesis. T_m = 643.15 K

selectivity and conversion is observed. However, the exact nature of the inverse relationship depends on the specific catalyst. At a particular conversion the propene selectivities vary as: 10VAl ∼ 3VTi > 2VTi > 7VNb > 1VTi. Thus, the nature of the propane conversion versus contact time and the inverse selectivity conversion relationship depends on the specific supported vanadium oxide catalyst. To learn more about the catalyst and to compare the catalysts properly it is necessary to estimate the kinetic parameters.

The kinetic parameters are estimated by varying the reaction temperature and propane to oxygen ratio for a Mars van Krevelan reaction model described above. It was observed that the values of CO_2 to CO ratio, ψ, used in the kinetic parameter estimation varies from 0.52 to 0.72 and are listed in the last column of Table 2. The value of ψ decreases somewhat with vanadia loading and the variations with oxide support appear minor. For the five catalysts the estimated kinetic parameters, k_{10}, k_{20}, k_{30}, E_1, E_2 and E_3, their units and the standard error associated with each kinetic parameter value are listed in Table 3. Comparison of the standard errors with the parameter values suggests that the kinetic parameters are estimated with a reasonable degree of accuracy. Additionally, a plot comparing the actual and predicted concentrations of the carbon containing compounds analyzed (CO, CO_2, C_3H_6 and C_3H_8) is given in Fig. 3 for the 7VNb catalyst. Fig. 3 reveals that a close correspondence exists between the actual and predicted concentrations. Similar plots are also observed for the other catalysts and are not shown for brevity suggesting that proper kinetic representation of the catalysts have been achieved.

Analysis of the kinetic parameters given in Table 3 reveals specific trends. For example, the pre-exponential factors, k_{10} and k_{20}, of the V_2O_5/TiO_2 catalysts increase monotonically as the loading is increased. The activation energy for propene formation, E_1, appears to decrease slightly with loading from 73 to 65 kJ/mol. The activation energy of propene decomposition, E_2, however, is relatively constant at 43–57 kJ/mol. Variations in the catalyst re-oxidation kinetic parameters, k_{30} and E_3, are addressed later. Since the propene formation activation energy decreases slightly the increase in k_{10} values with an increase in vanadia loading also implies an increase in k_1 values. To compare with the TOF data the k_{10} values given in Table 3 are normalized per vanadia site and represented by k^*_{10}. The k_1 or k_{10} values are related to the TOF by Eq. (8). The ratio of the k^*_{10} values reveal that $(k^*_{10})_{1VTi}:(k^*_{10})_{2VTi}:(k^*_{10})_{3VTi} \sim$ 1:1.8:2.5, where k^*_{i0} is given in terms of ml STP min^{-1} $_{(g\ V)}{}^{-1}$ atm^{-1}. With slightly decreasing activation energies the normalized rate constant k^*_1 values also vary similarly. However, the ratio of TOF is different since the degree of reduction is not considered. The degree of reduction will be discussed later.

It is tempting at this point to correlate changes in the k_{10} and k_{20}, or k_1 and k_2 values with the different vanadia structures present as a function of loading though other factors may also be involved. For example, during propane ODH reaction propane adsorption is limited and may play a major role in understanding the effect of vanadia loading. The adsorption kinetics depends on the surface acidity/basicity of the catalyst, which is known to vary with loading for V_2O_5/TiO_2 and V_2O_5/Al_2O_3 catalysts [40,41]. The difference in propane adsorption is reflected in the k_{10} values and consequently the k_1 values. It appears that the increase in k_{10} with loading is related to differences in propane adsorption kinetics; a higher vanadia loading assisting propane adsorption and giving rise to higher k_{10} and k_1 value. This non-linear change in acidity/basicity may or may not be related to the different vanadia structures present

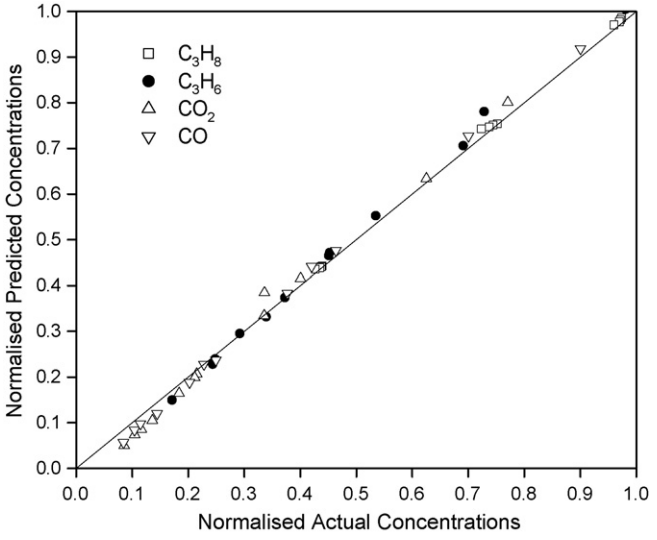

Fig. 3. Normalized predicted concentrations vs. normalized actual concentrations for 7VNb catalyst.

and the primary catalytic characteristic which is changing is the acidity/basicity. Thus, the k_{10} value increases with loading, which appear to be related to the increase in propane adsorption kinetics on the catalysts.

When the changes in support and loading are considered simultaneously the k_{10} values of the different catalysts vary as, $(k_{10})_{3VTi} > (k_{10})_{2VTi} > (k_{10})_{7VNb} > (k_{10})_{10VAl} \geq (k_{10})_{1VTi}$. The trend in the primary rate constant, k_1, would depend on the activation energies of propane conversion, E_1, which are not the same. The 10VAl sample possesses activation energy of 96 kJ/mol, which is higher than the 65–73 kJ/mol value observed for the other catalysts. Despite the differences in the activation energies for propane conversion the trend in k_1 and k_{10} values are the same. Normalizing the k_{10} values for the five catalysts as done previously reveals the following ratio, $(k_{10}^*)_{10VAl}:(k_{10}^*)_{7VNb}:(k_{10}^*)_{1VTi}:(k_{10}^*)_{2VTi}:(k_{10}^*)_{3VTi} \sim 1:2.3:6.8:12:17$. At 643 K the ratio of the normalized k_1 values, k_1^*, and k_{10}^* are the same since $T_m = 643$ K. The trends in the k_1^* values of the five catalysts correlates well with the trends in the TOF values mentioned above, however, the numerical values are different. As mentioned above for a quantitative comparison the degree of reduction specified in Eq. (8) is required and will be discussed later. Thus, the normalized primary rate constant of the surface vanadia site for propane oxidation, k_1^*, changes with loading and oxide support and is the largest when the support is TiO_2 and the least when the support is Al_2O_3. Furthermore, the k_1^* values, which represent the specific activity of the surface vanadia site for propane oxidation, differ by a factor of 13–20.5 for the 3VTi and 10VAl catalysts in the 613–673 K temperature range. The variation in the k_1^* values appear to be related to the inherent redox characteristics of the supported vanadia catalysts though the effect of acidity/basicity cannot be discounted [42]. It is expected that for a surface area of TiO_2 comparable to that of Al_2O_3 the k_1^* value can be further increased since a larger amount of surface vanadia can be accommodated.

The degree of reduction, β, is an important parameter to consider and is related to the rate constants, k_1 and k_2, and the partial pressures of propane, propene and oxygen. The degree of reduction for the five catalysts is evaluated by using Eq. (11) at 653 K and $C_3H_8:O_2$ ratio of 2:1 and shown in Fig. 4 as a function of contact time. From Fig. 4 it is evident that the degree of reduction depends on the contact time and catalyst. The variation of β with contact time is non-linear. Furthermore, at a particular contact time the degree of reduction, β, is the largest for the 3VTi and the least for the 10VAl catalyst. The primary reaction rate given by Eq. (8) depends on $(1-\beta)$. At a particular contact time of 75 kg m^{-3} s the $(1-\beta)$ values ratio of the different catalysts is $(1-\beta)_{10VAl}:(1-\beta)_{7VNb}:(1-\beta)_{1VTi}:(1-\beta)_{2VTi}:(1-\beta)_{3VTi} \sim 1.9:1.8:1.5:1.4:1$. Using the $k_1^*(1-\beta)$ values ratio improves the correspondence with the TOF ratio of the different catalysts mentioned above, however, a more quantitative description would involve the variation of the $P_{C_3H_8}(1-\beta)$ versus contact time since the variations are non-linear. Furthermore, the degree of reduction decreases the effective k_1 value differently for different catalysts. The effective k_1 value would correspond to pseudo-first order rate constants. Thus, the degree of reduction

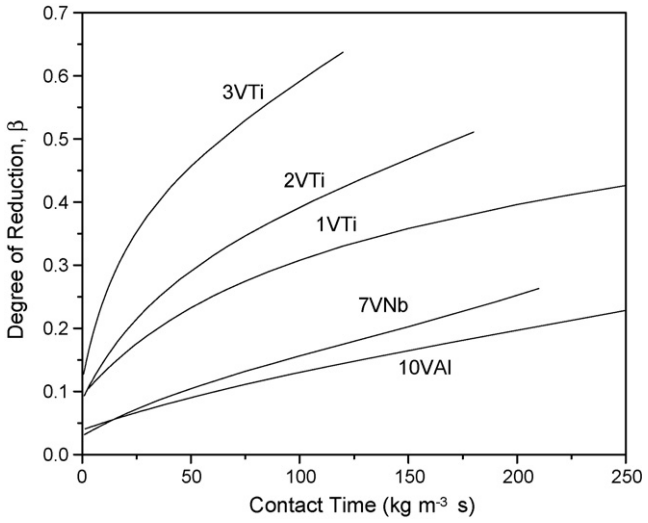

Fig. 4. Variation of degree of reduction with contact time for the different catalysts. $T = 653$ K and $C_3H_8:O_2 = 2:1$.

and its variation for each catalyst is important to consider when it is required to quantitatively correlate rate constants with the propane oxidation activity.

To understand the effect of different catalysts on the propene yield, variations in carbon oxides formation kinetic parameters, k_{20} and E_2, are also required. The propene yield at constant conversion for a sequence of first order reactions depends on the k_1/k_2 ratio [43]. The variation of the k_1/k_2 ratio for the different catalysts depends on the ratio of pre-exponential factors, k_{10}/k_{20}, and difference in activation energies, $E_1 - E_2$. These two parameters, k_{10}/k_{20} and $E_1 - E_2$, are also given in Table 3. Since the activation energy difference is relatively constant it is sufficient to study the variation k_{10}/k_{20} for the V_2O_5/TiO_2 catalysts. For the V_2O_5/TiO_2 catalysts the k_{10}/k_{20} value increases with loading since the value of k_{10} increases more rapidly than k_{20}. Experimentally, the propene yield at constant conversion also increases with loading for the V_2O_5/TiO_2 catalysts. It appears that the trend in k_1/k_2 ratio correlates well with the propene yield at constant conversion. Furthermore, the k_{10}/k_{20} values increases with vanadia loading and with a titania support possessing a surface area comparable to that of the present Al_2O_3 the k_{10}/k_{20} is expected to increase even further.

The importance of the k_1/k_2 ratio has been observed before [16,17]. It was suggested that the values of k_1/k_2 ratio can be increased by modifying the catalyst and/or increasing the temperature. For example, the k_{10} and k_{20} values decreased with phosphorous addition in V–P–O/TiO_2 catalysts; however, the relative change of the k_{10} and k_{20} values is different. It was observed that the k_{10}/k_{20} ratio increases since the k_{20} value decreases more rapidly compared to the k_{10} value. For the samples possessing similar activation energies, E_1 and E_2, the k_1/k_2 also increases with an increase in vanadium to phosphorous ratio. The k_1/k_2 ratio also increases with an increase in reaction temperature since $E_1 > E_2$.

When the oxide support is changed from TiO_2 to Nb_2O_5 the k_{10} and k_{20} values are between those for 1VTi and 2VTi. The k_{10}/k_{20} value for 7VNb is also between those for 1VTi and

2VTi. Since the activation energies for propene formation and degradation reactions of the 7VNb and V_2O_5/TiO_2 catalysts are comparable the k_1/k_2 value is also between those of 1VTi and 2VTi. For the 10VAl catalyst, however, the activation energy for propene formation, 96 kJ/mol, is larger and the activation energy of carbon oxide formation, 58 kJ/mol, is relatively similar to the values obtained for the V_2O_5/TiO_2 and V_2O_5/Nb_2O_5 catalysts. The activation energy difference, $E_1 - E_2$, is therefore largest for the 10VAl sample and the increase in propene formation at higher temperatures is more accentuated. Furthermore, the k_{10}/k_{20} ratio for the 10VAl sample is the highest of all the catalyst used in the present study. Thus, the trends in the k_1/k_2 values in the temperature range considered are: $(k_1/k_2)_{10VAl} > (k_1/k_2)_{3VTi} > (k_1/k_2)_{2VTi} > (k_1/k_2)_{7VNb} > (k_1/k_2)_{1VTi}$. As mentioned above the k_1/k_2 ratio values correlate well with the propene yields at iso-conversion over the V_2O_5/TiO_2 and previously determined V-P-O/TiO_2 series of catalysts. Extending this correlation to the 10VAl and 7VNb catalysts reveals that the correlation is still valid. The present results show that the propene yield or selectivity at iso-conversion varies as 10VAl ∼ 3VTi > 2VTi > 7VNb > 1VTi (see Fig. 2b), which is similar to the trend in k_1/k_2 variation observed. As mentioned above the k_1/k_2 ratio can also be changed by increasing the temperature. The predicted effect of varying the k_1/k_2 ratio by changing the catalyst and reaction temperature on the propene yield at 5% conversion levels is shown in Fig. 5. Fig. 5 reveals that increasing the k_1/k_2 ratio increases the propene yield. The increase in k_1/k_2 ratio is achieved by increasing the temperature or changing the catalyst. The overlapping nature of the curve for different catalysts demonstrates the importance of the k_1/k_2 ratio in determining the propene yield at iso-conversion. For example, the propene yield at 5% conversion can be increased by increasing the reaction temperature for the 1VTi catalyst. The increase in propene yield can also be achieved by a different catalyst, e.g., 10VAl, at a lower reaction temperature. The increase in propene yield at iso-conversion with increase in k_1/k_2 values is also reflected in the improvement of the inverse selectivity–conversion relationship as shown in Fig. 6 for the different catalyst. By changing the catalyst or by changing the temperature the k_1/k_2 ratio is changed and the simulated inverse selectivity–conversion can be tuned. Thus, the k_1/k_2 value correlates reasonably well with the trends in propene yields at iso-conversion and is an important parameter to consider for designing of an efficient propane ODH catalyst.

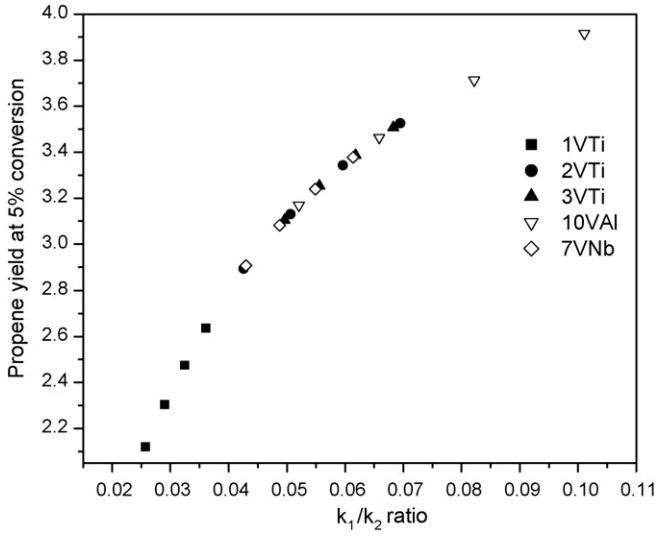

Fig. 5. Variation of propene yield at 5% conversion with k_1/k_2 ratio for the different catalysts. $C_3H_8:O_2 = 2:1$.

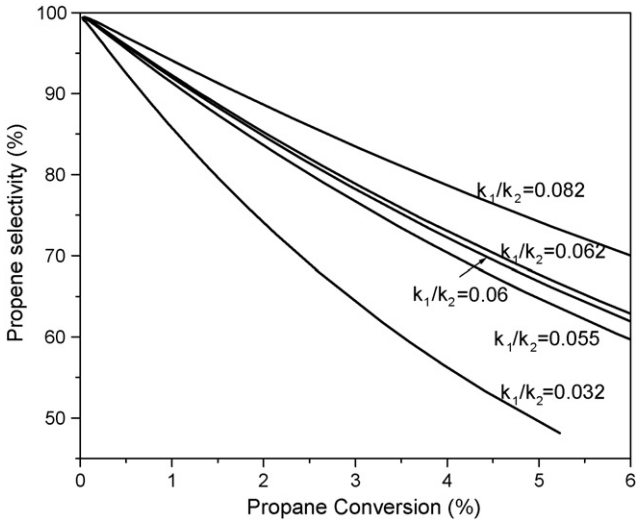

Fig. 6. The effect of k_1/k_2 ratio on the selectivity vs. conversion for propane ODH using kinetic parameters estimated. $T = 653$ K, $C_3H_8:O_2 = 2:1$.

The correlation between the propene yield and k_1/k_2 value is reasonable despite the reaction model not being first order and involves the degree of reduction, β, given in Eqs. (8)–(10). However, it should be noted that since $(1 - \beta)$ is involved in Eqs. (8) and (9) the effect of k_1/k_2 on the yield is independent of β provided comparisons are made at iso-conversions.

The specific vanadia loading on the different oxide supports also plays a significant role in designing a catalyst for obtaining high propene yields. Since the k_1/k_2 ratio is dimensionless normalizing in terms of vanadia loading imparts little meaning. Since the alumina support has a higher surface area the vanadia loading required for monolayer coverage is significantly higher. The monolayer coverage in terms of vanadium atoms per nm^2 is, however, independent of these specific oxide-supports [44]. To take into consideration the varying surface area and consequently the varying surface coverage of the catalysts the predicted and actual propene yields are plotted versus vanadia loading-based contact time, kg V $(m^3)^{-1}$ s, in Fig. 7. Comparison at the same vanadia loading-based contact time would reflect the effective propene yield capacity of the surface vanadia site on each of the catalysts. Comparing at the same vanadia loading-based contact time from Fig. 7 suggests that the propene yield varies with loading (see for example the VTi series) and the oxide support. The trend in propene yield at the same vanadia loading-based contact time is as follows: 3VTi > 2VTi > 1VTi > 7VNb > 10VAl. This trend suggests that propene yields are the highest for the surface vanadia site on titania, followed by niobia and finally alumina. The implications of this analysis is that on similar surface areas of

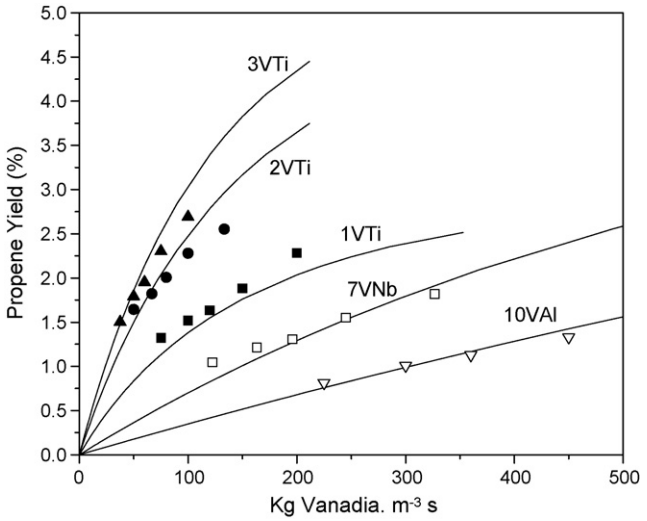

Fig. 7. Variation of propene yield vs. vanadia-loading based contact time. Symbols are experimental points and lines are predicted values. $T = 653$ K, $C_3H_8{:}O_2 = 2{:}1$.

the oxide supports the surface vanadium oxide species on TiO_2 would be the most beneficial to produce propene followed by Nb_2O_5 and then Al_2O_3. Since the Al_2O_3 surface area was the highest a larger amount of surface vanadia is accommodated giving rise to high k_1/k_2 values and propene yields. Increasing the TiO_2 surface area to values equivalent to the Al_2O_3 support would increase the vanadia loading to achieve monolayer coverages, which would increase the k_1/k_2 value further and also the propene yields. The propane conversion at iso-contact times would also increase since now the monolayer limits would be achieved at a higher vanadia loading. Thus, using a TiO_2 support possessing higher surface area would assist in increasing the propane conversion and propene yield. Care must be taken, however, to ensure that the high surface area V_2O_5/TiO_2 catalyst will be thermally stable at similar reaction conditions.

The effect of the vanadia loading and oxide support on the kinetic parameters associated with the re-oxidation reaction, k_{30} and E_3, is also observed. The k_{30} values increase with loading for the V_2O_5/TiO_2 catalysts. The vanadium normalized k^*_{30} values are lowest for the V_2O_5/Al_2O_3 followed by the V_2O_5/Nb_2O_5 and then the V_2O_5/TiO_2 catalysts. The re-oxidation activation energy for Nb_2O_5 supported samples is the largest, 171 kJ/mol, followed by TiO_2 supported samples, 136–144 kJ/mol, and the Al_2O_3 supported sample is the least, 117 kJ/mol.

4. Conclusions

Supported vanadium oxide catalysts were synthesized and characterized to understand the effect of vanadia loading and oxide support on the propane ODH reaction. The characterization techniques reveal that only surface vanadia species were present. Contact time studies suggest that the propane oxidation TOF is independent of loading and the propene yield depends on loading and oxide support. The effect of vanadia loading and oxide support on the reaction was determined by studying the kinetic parameters estimated for a sequential Mars van Krevelan reaction mechanism. The kinetic parameters determined were the pre-exponential factors, k_{i0}, and activation energies, E_i, for the propene formation or propane oxidation, carbon oxides formation or propene degradation and catalyst re-oxidation reactions. The kinetic parameters were able to predict the observed outlet concentrations of all carbon containing compounds and were found to vary with vanadia loading and the oxide support used to form the surface vanadia species. The pre-exponential factors for the propane oxidation and propene decomposition reaction, k_{10} and k_{20}, increased monotonically with vanadia loading for the series of V_2O_5/TiO_2 catalysts. However, the activation energies for the two reactions, E_1 and E_2, were relatively independent of loading. Furthermore, E_2 was relatively independent of the oxide support used to form the surface vanadia species. The E_1 value was, however, different for the V_2O_5/Al_2O_3 catalyst. To simultaneously compare the effect of the oxide support and loading it was necessary to normalize the pre-exponential factors based on the vanadia content. The normalized pre-exponential factor for propane oxidation varied with loading for the V_2O_5/TiO_2 series of catalysts. The normalized pre-exponential factor for propane oxidation also varied with the oxide support and was found to be the largest for the V_2O_5/TiO_2 catalysts followed by the V_2O_5/Nb_2O_5 catalyst and finally the V_2O_5/Al_2O_3 catalyst. The ratio of rate constant for propane oxidation correlates well with the trends in propane oxidation TOF, however, a quantitative correlation requires that the degree of reduction should also be considered. The propene yield at iso-conversion correlates well with the rate constant ratio for propene to carbon oxides formation, k_1/k_2. Since the k_1/k_2 value is the highest for the V_2O_5/Al_2O_3 catalyst the propene yield at iso-conversion is also the highest amongst the catalysts considered in the present study. However, the propene yield at the same vanadia-loading based contact time is the highest for the V_2O_5/TiO_2 catalysts followed by the V_2O_5/Nb_2O_5 and finally the V_2O_5/Al_2O_3 catalyst. The results from the propene yields at the same vanadia-loading based contact time suggest that a higher surface area titania will assist in improving the propene yields by increasing the k_1/k_2 ratio. Consequently, the selectivity–conversion relationship will also be improved. Furthermore, using a higher surface area titania support will increase the propane oxidation activity, by increasing the k_1 value. Thus, using a higher surface area titania will assist in designing a better catalyst for propane conversion and improving the selectivity–conversion relationship.

Acknowledgement

The authors would like to gratefully acknowledge Prof. Israel E. Wachs, Lehigh University, Bethlehem, PA, USA, for allowing us to obtain the Raman spectra on some of the catalyst.

References

[1] E.A. Mamedov, V.C. Corberan, Appl. Catal. A Gen. 127 (1995) 1.
[2] F. Genser, S. Pieterzyk, Chem. Eng. Sci. 54 (1999) 4315.

[3] R. Grabowski, B. Grzybowska, K. Samson, J. Sloczynski, J. Stoch, K. Weislo, Appl. Catal. A Gen. 125 (1995) 129.
[4] A. Parmaliana, V. Sokolovski, M. Danial, N. Giordano, Appl. Catal. A Gen. 135 (1996) L1.
[5] F. Arena, F. Frusteri, A. Parmalian, Catal. Lett. 60 (1999) 59.
[6] A.A. Lemonidou, L. Nalbandian, I.A. Vasalos, Catal. Today 61 (2000) 333.
[7] G. Martra, F. Arena, S. Coluccia, F. Frusteri, A. Parmaliana, Catal. Today 63 (2000) 197.
[8] A. Khodakov, B. Olthof, A.T. Bell, E. Iglesia, J. Catal. 181 (1999) 205.
[9] K. Chen, A. Khodakov, J. Yang, A.T. Bell, E. Iglesia, J. Catal. 186 (1999) 325.
[10] K. Routray, K.R.S.K. Reddy, G. Deo, Appl. Catal. A Gen. 265 (2004) 103.
[11] M. De, D. Kunzru, Catal. Lett. 96 (2004) 33.
[12] X. Gao, J.M. Jehng, I.E. Wachs, J. Catal. 209 (2002) 43.
[13] A. Bottiono, G. Capabnnelli, A. Comite, S. Storace, R.D. Felice, Chem. Eng. J. 94 (2003) 11.
[14] T.S.L. Anderson, Appl. Catal. A Gen. 112 (1994) 209.
[15] R. Grabowski, J. Sloczynski, N.M. Grzesik, Appl. Catal. A Gen. 242 (2003) 297.
[16] K. Routray, G. Deo, AIChE J. 51 (2005) 1733.
[17] R.P. Singh, M.A. Banares, G. Deo, J. Catal. 233 (2005) 388.
[18] T.C. Walting, G. Deo, K. Seshan, I.E. Wachs, J.A. Lercher, Catal. Today 28 (1996) 139.
[19] H. Tian, L.E. Briand, I.E. Wachs, J. Phys. Chem. B 109 (2005) 23491.
[20] G.E.P. Box, N.R. Draper, Biometrika 52 (1965) 355.
[21] S. Vajda, P. Valko, Comp. Chem. Eng. 10 (1) (1986) 49.
[22] R. Mezaki, J.B. Butt, I&EC Fundam. 7 (1) (1968) 120.
[23] G.F. Froment, K.B. Bischoff, Chemical Reactor Analysis and Design, second ed., Wiley, New York, 1990.
[24] G.E.P. Box, W.G. Hunter, J.F. MacGregor, J. Erjavec, Technometrics 15 (1973) 33.
[25] Kangal: http://www.iitk.ac.in/kangal/soft.htm.
[26] D.G. Watts, Can. J. Chem. Eng. 72 (1994) 701.
[27] D.J. Pritchard, D.W. Bacon, Chem. Eng. Sci. 33 (1978) 1539.
[28] N. Brauner, M. Shacham, Chem. Eng. Process. 36 (1997) 243.
[29] N. Magg, B. Immaraporn, J.B. Giorgi, T. Schroeder, M. Baumer, J. Dobler, Z. Wu, E. Kondratenko, M. Cherian, M. Baerns, P.C. Stair, J. Sauer, H.J. Freund, J. Catal. 226 (2004) 88.
[30] I.E. Wachs, Y. Chen, J.M. Jehng, L.E. Briand, T. Tanaka, Catal. Today 78 (2003) 13.
[31] G. Deo, F.D. Hardcastle, M. Richards, A.M. Hirt, I.E. Wachs, Novel materials in heterogeneous catalysis, in: R.T.K. Baker, L.L. Murrell (Eds.), ACS Symposium Series, vol. 437, American Chemical Society, Washington, DC, 1990, p. 317.
[32] H. Eckert, I.E. Wachs, J. Phys. Chem. 93 (1989) 6796.
[33] N.R. Shiju, M. Anilkumar, S.P. Mirajkar, C.S. Gopinath, B.S. Rao, C.V. Satyanarayana, J. Catal. 230 (2005) 484.
[34] G. Deo, I.E. Wachs, J. Phys. Chem. 95 (1991) 5889.
[35] M.A. Vuurman, I.E. Wachs, A.M. Hirt, J. Phys. Chem. 95 (1991) 9928.
[36] M.A. Vuurman, I.E. wachs, J. Mol. Catal. 77 (1992) 29.
[37] B. Weckhuysen, J.M. Jehng, I.E. Wachs, J. Phys. Chem. B 101 (1996) 2793.
[38] Z. Zhao, X. Gao, I.E. Wachs, J. Phys. Chem. B 107 (2003) 6333.
[39] J.G. Eon, R. Olier, J.C. Volta, J. Catal. 145 (1994) 318.
[40] M.D. Amiridis, R.V. Duevel, I.E. Wachs, Appl. Catal. B Environ. 20 (1999) 111.
[41] A.M. Turek, E.D. Canio, I.E. Wachs, J. Phys. Chem. 96 (1992) 5000.
[42] G. Deo, I.E. Wachs, J. Haber, Crit. Rev. Surf. Chem. 4 (1994) 141.
[43] H.S. Fogler, Elements of Chemical Reaction Engineering, third ed., Prentice-Hall of India Pvt. Ltd., New Delhi, 2002, p. 292.
[44] I.E. Wachs, Catal. Today 27 (1996) 437.